Pantograph Catenary Contact Force Regulation Based on Modified Takagi-Sugeno Fuzzy Models

Nguyen Van Hai
Department of Electrical Engineering, University of Transport and Communications, Vietnam
haiktd@utc.edu.vn
(corresponding author)

Nguyen Van Tiem
Department of Cybernetics, University of Transport and Communications, Vietnam
nguyenvantiem@utc.edu.vn

Le Hung Lan
Department of Cybernetics, University of Transport and Communications, Vietnam
lehunglan@utc.edu.vn

Vo Thanh Ha
Department of Cybernetics, University of Transport and Communications, Vietnam
vothanhha.ktd@utc.edu.vn

Received: 27 October 2022 | Revised: 9 November 2022 | Accepted: 10 November 2022

ABSTRACT

In this paper, a new contact force control technique, based on the modified Takagi-Sugeno model and the parallel distributed compensation concept is developed to suppress vibrations between the pantograph and the catenary by regulating the contact force to a reference value, thereby achieving stable current collection. The proposed method uses simple and standard PID and modified Takagi-Sugeno fuzzy controllers. The two controllers guarantee the designed system's robust stability. Furthermore, based on a simplified pantograph–catenary system model, the comparative simulation results show that variations of the contact force can be almost attenuated. As a result, the system stability is guaranteed, and the performance robustness is verified.

Keywords-Takagi-Sugeno; pantograph; catenary; stability; modified T-S-Fuzzy

I. INTRODUCTION

Improving the current collection quality from the overhead line is one of the most challenging difficulties in high-speed rails. The pantograph, an articulated suspension device, ensures the overhead line's current collection, but its interaction with the contact wire results in oscillations. This system must guarantee a good quality of the existing collection, it must thus be compensated. This issue mainly affects expensive railroads because poor current collection results in performance constraints, high maintenance cost, and inconsistent service. The pantograph-catenary system, a dynamic couple system formed by the interactions of the pantograph and catenary, is often responsible for directly affecting the quality of electric transmission (PCS). Through contact forces, the pantograph and the catenary are impacted by one another. The overhead wire's varying stiffness along the span [1-4] is a significant cause of vibration. The pantograph will vibrate and the contact force will fluctuate as it moves along the overhead wire due to the stiffness change those results in a periodic excitation. Additionally, while a moving panhead travels along the overhead wire, a flexural wave motion is created in the wire, affecting the contact force and motion pantograph. An actuator, an essential component of the PCS, applies the dynamic uplift force to the pantograph frame within the context of the active vibration control of a railway pantograph to significantly reduce the contact force's unpredictable fluctuation. Many control algorithms have been developed (simple PI controllers [5], robust controllers [6], adaptive controllers [7], backstepping controllers [8], predictive model controllers [9], intelligent controllers [10–12], and fuzzy controllers [13]) for producing adequate uplift force to regulate the fluctuation of the contact force. To manage the oscillations brought on by the unpredictable stiffness and to regulate the contact force taken into account as a pre-specified reference value, an intelligent contact force regulator, including MZL algorithms [14-15], is given in [10]. The vibration of the contact force caused by the catenary's time-varying stiffness can be successfully suppressed, and the comparative simulation results demonstrate that the suggested method is more effective than the previous fuzzy algorithms. However, although intelligent or fuzzy control are promising techniques, there are still issues with constructing ambiguous regulations and ensuring system stability. The Parallel Distributed Compensation (PDC) idea and the modified Takagi-Sugeno (T-S) model are the foundations of the contact force control approach proposed in this work. Furthermore, the devised technique enables the execution of straightforward and joint PID controllers to ensure the robust stability of the proposed system.

II. PROBLEM FORMULATION

The model of the pantograph – catenary system is exhibited in Figure 1. It is represented by a 2-degree of freedom mechanical system as shown in Figure 2. The motion equation of the PCS model can be written as [12]:

$$\begin{aligned} &m_h \ddot{x}_h + c_h(\dot{x}_h - \dot{x}_f) + k_h(x_h - x_f) + k_{pan}(x_h - x_{cat}) = 0 \\ &k_{pan}(x_{cat} - x_h) + k_{cat}x_{cat} = 0 \\ &m_f \ddot{x}_f - c_h(\dot{x}_h - \dot{x}_f) + c_f \dot{x}_f - k_h(x_h - x_f) = u \end{aligned} \tag{1}$$

or:

$$\begin{aligned} &m_h \ddot{x}_h + c_h(\dot{x}_h - \dot{x}_f) + k_h(x_h - x_f) + k_0 x_h = 0 \\ &m_f \ddot{x}_f - c_h(\dot{x}_h - \dot{x}_f) + c_f \dot{x}_f - k_h(x_h - x_f) = u \end{aligned} \tag{2}$$

where:

$$k_0 = \frac{k_{pan}k_{cat}}{k_{pan} + k_{cat}} \tag{3}$$

By taking the Laplace transformation of (2), one gets:

$$\begin{aligned} &\left[m_h s^2 + c_h s + (k_h + k_0)\right]X_h(s) - (c_h s + k_h)X_f(s) = 0 \\ &-(c_h s + k_h)X_h(s) + \left[m_f s^2 + (c_f + c_h)s + k_h\right]X_f(s) = U(s) \end{aligned} \tag{4}$$

where the term s is defined as: $X_h(s) = \frac{F(s)}{k}$. For that, the plant transfer function $P(s)$ can be computed as follows:

$$P(s) = \frac{F(s)}{U(s)} = \frac{k(c_h s + k_h)}{M(s)} \tag{5}$$

where:

$$\begin{aligned} M(s) &= \left[m_f s^2 + (c_f + c_h)s + k_h\right]\left[m_h s^2 + c_h s + (k_h + k_0)\right] \\ &-(c_h s + k_h)^2 = m_f m_h s^4 + \left[m_f c_h + (c_f + c_h)m_h\right]s^3 \\ &+\left[m_f(k_h + k_0) + m_h k_h + c_h c_f\right]s^2 \\ &+\left[k_0(c_f + c_h) + k_h c_f\right]s + k_h k_0 \end{aligned} \tag{6}$$

It should be noted that the dynamic uplift force $u(t)$ is designed to regulate the contact force $F(t)$ for the prescribed constant value $F_r(t)$=100N. If the time-varying stiffness of the catenary influenced by the stiffness variation coefficient a, the operational speed of the train V, and the length in a span L are considered, the contact force $f(t) = kx_h(t)$ will be rewritten as:

$$f(t) = k_0\left(1 + \alpha\cos(\frac{2\pi V}{L}t)\right)x_h(t) \tag{7}$$

where:

$$k = k_0\left(1 + \alpha\cos(\frac{2\pi V}{L}t)\right) \tag{8}$$

Clearly, the term of k can be considered as an uncertain interval parameter $k \in \left[k_{min}, k_{\max}\right]$, which can be expressed as:

$$k_{min} = k_0(1-\alpha),\ k_{max} = k_0(1+\alpha) \tag{9}$$

where m_h is the head mass, m_f the frame mass, x_h and x_f the head displacement, k_h the head stiffness of suspension, c_h the head viscous damping coefficient, c_f the frame viscous damping coefficient, k_{pan} the pantograph shoe stiffness of suspension, k_{cat} the catenary stiffness of suspension, and u the uplift force.

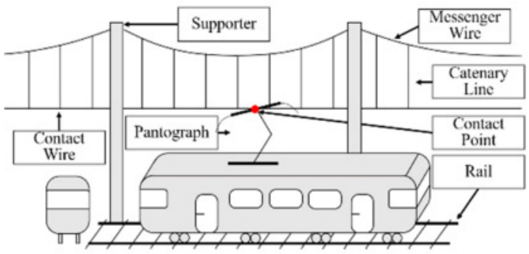

Fig. 1. Pantograph–catenary system components.

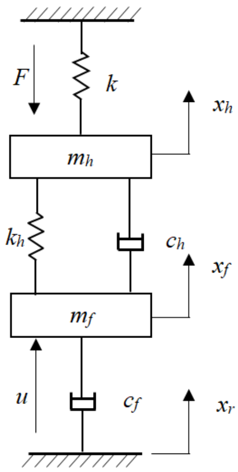

Fig. 2. The PCS 4th order model.

In this paper, stable robust controllers are developed to suppress the vibration resulting from parameters (the stiffness-variation coefficient a, the operational speed of train V and the length in a span L). The first solution is the robust PI controller, and the second one is the T-S fuzzy controller. Both solutions are based on the most common industrial controller, the PID controller. The parameters of the PCS used in the simulation [12] are: $m_h = 9.1\text{kg}$, $m_f = 17.2\text{kg}$, $k_h = 7x10^3\,\text{N/m}$, $c_h =$ 130Ns/m, $c_f = 30\text{Ns/m}$, $k_{cat} = 1.535x10^6\,\text{N/m}$, $\alpha = 0.3$, $k_{pan} = 8.23\times10^4\,\text{N/m}$, $V = 70\text{km/h}$, $L = 80\text{m}$, and for the given parameters, the following values are respectively computed: $k_{\min} = 54678$, $k_{\max} = 101550$.

III. PARTITION METHOD

The PI controller is given as:

$$C(s) = K_P + \frac{K_I}{s} \tag{10}$$

Then the closed loop transfer functions of (5) and (10) can be written as:

$$\text{W}(s) = \frac{C(s)P(s)}{1+C(s)P(s)} = \frac{k(K_P s + K_I)(c_h s + k_h)}{sM(s) + k(K_P s + K_I)(c_h s + k_h)} \tag{11}$$

where $k \in \left[k_{min}, k_{\max}\right]$.

The closed loop system characteristic equation is defined as:

$$H(s) = sM(s) + k(K_P s + K_I)(c_h s + k_h) \tag{12}$$

where:

$$M(j\omega) = R_M(\omega) + jI_M(\omega) \tag{13}$$

Based on the robust D-partition technique [15], it can be seen that the stability region boundary in the $K_P - K_I$ space is the solution of the following equation:

$$\begin{aligned} H(j\omega) = &\left[k(k_h K_I - c_h\omega^2 K_P) - \omega I_M(\omega)\right] \\ &+ j\left[k\omega(K_P k_h + K_I c_h) + \omega R_M(\omega)\right] \end{aligned} \tag{14}$$

Equation (14) is equivalent to:

$$-kc_h\omega^2 K_P + kk_h K_I = \omega I_M(\omega) \tag{15}$$

where the functions are respectively expressed as:

$$\begin{aligned} K_P &= -\frac{\omega c_h I_M(\omega) + k_h R_M(\omega)}{k(c_h^2\omega^2 + k_h^2)} \\ K_I &= -\frac{\omega[c_h\omega R_M(\omega) - k_h I_M(\omega)]}{k\omega(c_h^2\omega^2 + k_h^2)} \end{aligned} \tag{16}$$

In (16), when ω varies from 0 to ∞, the obtained values of K_p and K_I are considered as the stability region boundary in the form of the single curve for a specific value of k. This boundary will be the group of curves when k varies within the interval $k \in \left[k_{min}, k_{\max}\right]$. The robust stability region for the given PCS is shown in Figure 3.

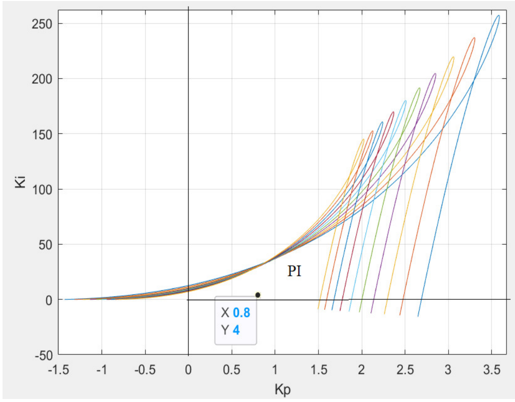

Fig. 3. Robust stability region of the PI controller.

IV. MODIFIED T-S-FUZZY CONTROLLER

The T-S model is one of the most well-liked modeling frameworks among the different fuzzy modeling topics [16-17]. Since it can approximate any smooth nonlinear control system, the T-S fuzzy model is considered a universal approximator. Additionally, several feedback control strategies may be used with T-S fuzzy models. The PDC idea is the foundation for the control law that is most frequently employed, and for this concept, the fuzzy controller and T-S fuzzy model share the same fuzzy rules and sets [18]. A linear controller is created for each local linear plant by the PDC principle to provide stability and the desired performance of the local linear closed loop system, compensating a corresponding conclusion in the rules of the T-S plant model. The final nonlinear control is an amorphous amalgamation of the many regulations and control operations. Finding a combined Lyapunov function that can satisfy all fuzzy subsystems results in a sufficient condition that guarantees the entire system's stability. To determine the well-known Lyapunov role, Linear Matrix Inequalities (LMIs) must be solved numerically. The primary downsides of the PDC design technique are the complexity of the computations without a solution guarantee and the difficulty in locating the combined Lyapunov function for the numerous fuzzy subsystems. To address these problems, a novel fuzzy logic controller with two consequents in each rule—a numerator component and a denominator part—is presented in [19].

Additionally, the numerator and denominator coefficients are calculated so that the total closed-loop system acts as a linear system. Further, the notion above is expanded for continuous systems in the suggested method in [14]. The closed-loop T-S fuzzy control system acts as a polytope of linear systems based on the recently developed technique. Instead of employing a problematic method to find a joint Lyapunov function as in the previous approaches, the system stability may be readily tested using simple, graphical solid stability criteria.

First of all, the interval [k_{min}, k_{max}] is divided into r overlapping subintervals. The linear subintervals are defined as the fuzzy sets and form the universe of discourse. The r+2 triangular membership functions corresponding to the subintervals of the following form are presented in Figure 4.

For each i-th interval, a represented value k_i is chosen. For that, a fuzzy variable M_i with the related membership functions μ_i is defined. Furthermore, the two interval boundaries of k_{min} and k_{max} are also added. For the correspondence of the i-th interval, the local plant transfer function can be obtained.

$$P_i(s)=\frac{F(s)}{U(s)}=\frac{k_i(c_h s+k_h)}{M(s)},\ i=1,...,r+2 \tag{17}$$

where the function $M(s)$ is defined as:

$$\begin{aligned}M(s) &= m_f m_h s^4+\left[m_f c_h+(c_f+c_h)m_h\right]s^3\\ &+\left[m_f(k_h+k_0)+m_h k_h+c_h c_f\right]s^2\\ &+\left[k_0(c_f+c_h)+k_h c_f\right]s+k_h k_0\end{aligned} \tag{18}$$

We also have:

$$\begin{aligned}&c_1^i=\frac{k_i c_h}{m_h m_f},\ c_0^i=\frac{k_i k_h}{m_h m_f},\\ &d_3^i=\frac{m_f c_h+(c_f+c_h)m_h}{m_h m_f},\\ &d_2^i=\frac{\left[m_f(k_h+k_0)+m_h k_h+c_h c_f\right]}{m_h m_f},\\ &d_1^i=\frac{k_0(c_f+c_h)+k_h c_f}{m_h m_f},\ d_0^i=\frac{k_h k_0}{m_h m_f}\end{aligned} \tag{19}$$

The local transfer function in (17) will be then expressed as:

$$P_i(s)=\frac{F(s)}{U(s)}=\frac{c_1^i s+c_0^i}{s^4+d_3^i s^3+d_2^i s^2+d_1^i s+d_0^i} \tag{20}$$

or in the form of the following differential equation:

$$\begin{aligned}&f^{(5)}(t)=-d_3^i f^{(4)}(t)-d_2^i f^{(3)}(t)\\ &-d_1^i f^{''}(t)-d_0^i f^{'}(t)+c_1^i u^{''}(t)+c_0^i u^{'}(t)\end{aligned} \tag{21}$$

For each above local plant, the local PI controller is used:

$$C_i(s)=\frac{U(s)}{E(s)}=K_P^i+\frac{K_I^i}{s}=\frac{K_P^i s+K_I^i}{s},\ i=1,...,r+2 \tag{22}$$

or, in the form of the following differential equation:

$$\begin{aligned}&c_1^i u^{''}(t)+c_0^i u^{'}(t)=-k_P^i c_1^i f^{''}(t)\\ &-(k_P^i c_0^i+k_I^i c_1^i)f^{'}(t)-k_I^i c_0^i f(t)+k_I^i c_0^i f_r\end{aligned} \tag{23}$$

The local PI controller parameters can be finally chosen by using the proposed robust D-partition and some optimal performance criterions. By using the modified fuzzy T-S model [14-15], the i-th fuzzy IF-THEN rule for the describing plant is presented as follows:

1) *Plant Model Rule* R_i: $i=1,...,r+2$
IF $k(t)$ is M_i THEN

$$\begin{aligned}&f^{(5)}(t)=-d_3^i f^{(4)}(t)-d_2^i f^{(3)}(t)\\ &-d_1^i f^{''}(t)-d_0^i f^{'}(t)+c_1^i u^{''}(t)+c_0^i u^{'}(t)\end{aligned} \tag{24}$$

where R_i is denoted as the i-th fuzzy inference rule, r is the number of inference rules, and $M_i\,(i\in\Omega_r)$ is the fuzzy set.

The PDC design approach creates a control rule based on the same presumption with each rule in the T-S fuzzy plant model. A numerator component and a denominator part of the control signal are the two consequents each control rule of the fuzzy logic controller has in its consequent section [19] part and a denominator part of the control signal [20-21].

2) *Control Rule* R_i, $i=1, ...r+2$
IF $k(t)$ is M_i THEN

$$\begin{aligned}&num\,u^{'}(t)=-K_P^i c_1^i f^{''}(t)-(K_P^i c_0^i+K_I^i c_1^i)f^{'}(t)\\ &-K_I^i c_0^i f(t)+K_I^i c_0^i f_r-c_1^i u^{''}(t)\\ &den\,u^{'}(t)=c_0^i\end{aligned} \tag{25}$$

where $num\,u^{'}(t)$ is the numerator of $u^{'}(t)$ and $den\,u^{'}(t)$ is the denominator of $u^{'}(t)$.

The closed loop system characteristic function is:

$$\begin{aligned}&s^5+\sum_{i=1}^{r}h_i(k)d_3^i s^4+\sum_{i=1}^{r}h_i(k)d_2^i s^3\\ &+\sum_{i=1}^{r}h_i(k)(d_1^i+K_P^i c_1^i)s^2\\ &+\sum_{i=1}^{r}h_i(k)(d_0^i+K_P^i c_0^i+K_I^i c_1^i)s\\ &+\sum_{i=1}^{r}h_i(k)K_I^i c_0^i=0\end{aligned} \tag{26}$$

where $h_i(k)$ is the normalized membership function. It should be noted that the normalized membership functions satisfy the following convex sum property:

$$0\le h_i(k)\le 1,\ i=1,...,r+2,\ \sum_{i=1}^{r+2}h_i(k)=1 \tag{27}$$

The left-hand side of (27) is the characteristic polynomial, and it is actually the polytope of polynomials:

$$H(s)=\sum_{i=1}^{r+2}h_i(z)H_i(s), \tag{28}$$

$$0\le h_i(z)\le 1, i=1,...,r+2,\ \sum_{i=1}^{r+2}h_i(k)=1$$

where:

$$\begin{aligned}&H_i(s)=s^5+d_3^i s^4+d_2^i s^3+(d_1^i+K_P^i c_1^i)s^2\\ &+(d_0^i+K_P^i c_0^i+K_I^i c_1^i)s+K_I^i c_0^i\end{aligned} \tag{29}$$

Therefore, system stability analysis can be conducted by using the robust stability criteria [18-19], derived in [14].

3) *Theorem*

The fuzzy closed loop system (21), (22) is stable if and only if:

- The polynomials $H_i(s),\ i=1,...,r+2$ are stable.
- All $\frac{(r+1)(r+2)}{2}$ plots, $z_{ij}(\omega)=\dfrac{H_i(j\omega)}{H_j(j\omega)},\ i,j=1,...,r+2,\ i<j$ do not intersect the negative real semi axis.

V. SIMULATION RESULTS

The system simulation model simulated in MATLAB R2019a includes three parts, i.e. the open-loop system (no control), one system using the robust PI controller, and one using the new T-S fuzzy controller. The control construct of contact force regulation of the pantograph catenary based on modified T-S Fuzzy models is shown in Figure 4.

1) *Case 1. Robust PI Controller*

For an example of the given PCS, the robust stability region of PI controller is found in Figure 3. The typical PI controller parameters in this region can be determined as: $K_P=0.8,\ K_I=4$

2) *Case 2. Modified T-S Fuzzy Controller*

First, the interval $\left[k_{min},k_{max}\right]$ is divided into $r=4$ overlapping subintervals with triangular membership functions as pointed out in Figure 5.

By using the proposed D-partition method, the robust stability regions for each subinterval can be constructed, and the local PI controller parameters can be chosen inside those regions:

$$K_P^1=K_P^2=K_P^3=K_P^4=K_P^5=K_P^6=0.1$$

$$K_I^1=4.968,\ K_I^2=4.241,\ K_I^3=3.7,\ K_P^4=3,281,\ K_I^5=2.947,\ K_I^6=2.675.$$

Next, the two conditions in the given theorem are verified by using 6 Mikhailov's graphs $H_i(j\omega)$ (Figure 6) and 15 $z_{ij}(j\omega)$ graphs as shown in Figure 7.

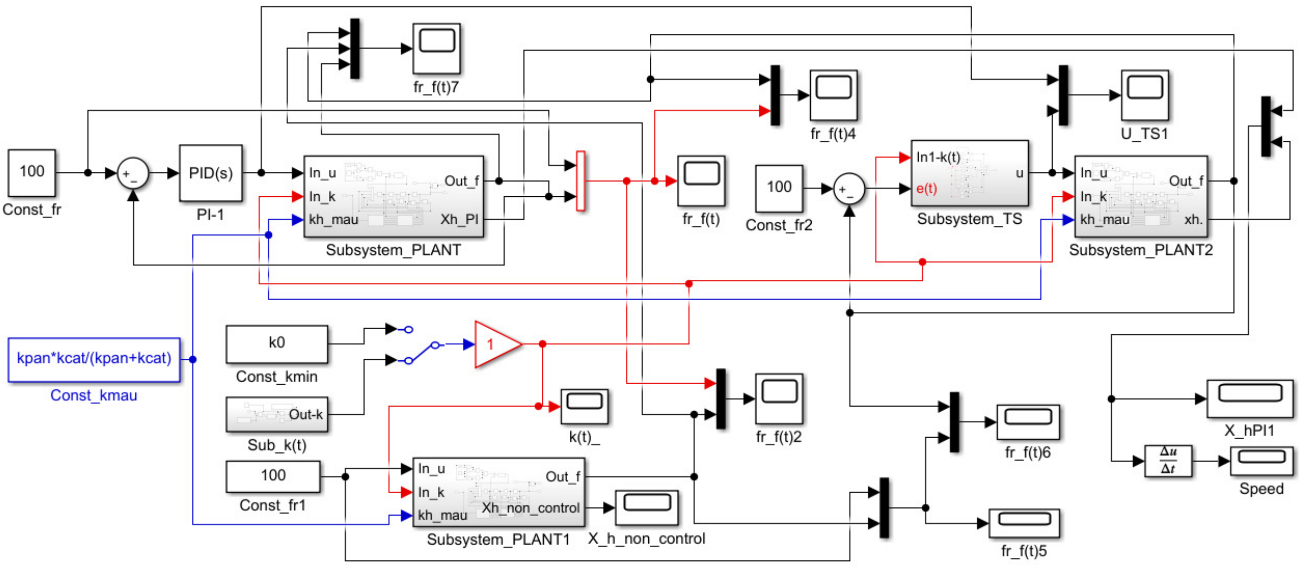

Fig. 4. The control construct of contact force regulation of pantograph catenary based on modified Takagi-Sugeno Fuzzy model.

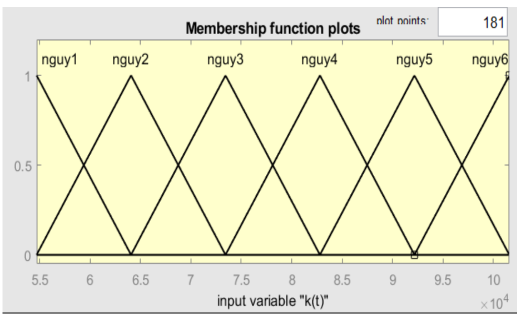

Fig. 5. The triangular membership functions.

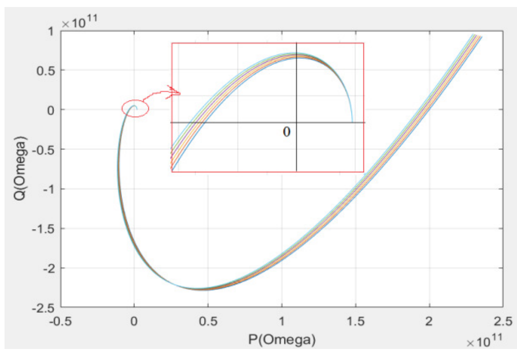

Fig. 6. Mikhailov's graphs.

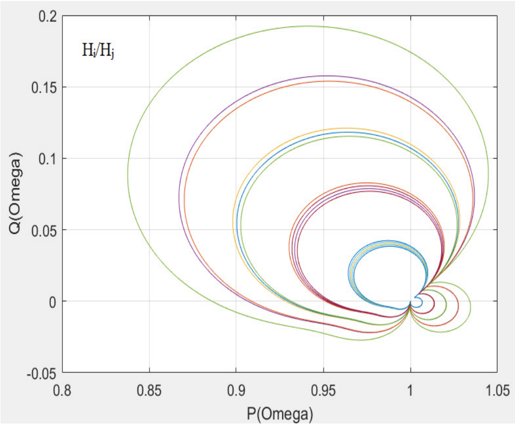

Fig. 7. Graphs $z_{ij}(j\omega)$.

(a)
(b)

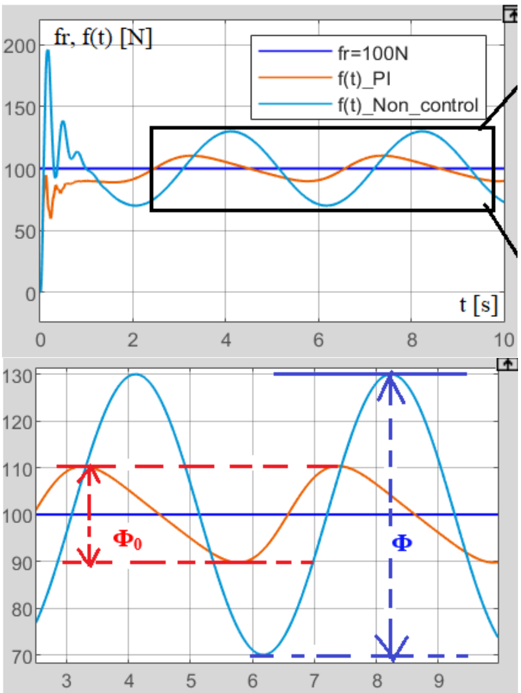

Fig. 8. Contact force regulation performance of the robust PI algorithm.

Now let us consider a closed-loop control system, which consists of the plant described by (5) and the fuzzy controller of (25). In order to verify the regulation performance, the two control algorithms proposed in this paper have been analyzed and compared with passive control and MZL algorithm in [12], or each with other using the vibration suppression efficiency (VSE) [12]:

$$VSE \triangleq \left(1-\frac{\Phi}{\Phi_0}\right)100\% \quad (27)$$

where Φ is the amplitude of the steady contact force value and $\Phi_0 = 2\alpha f_r(t)$ is the amplitude of the contact force by the traditional passive control.

By applying the robust PI controller, the graph of contact force shown in Figure 8 is defined with *VSE*=65.6617%. When using the proposed modified T-S fuzzy controller, the graph of contact force presented in Figure 9 is determined with VSE=97.68%.

(a)
(b)

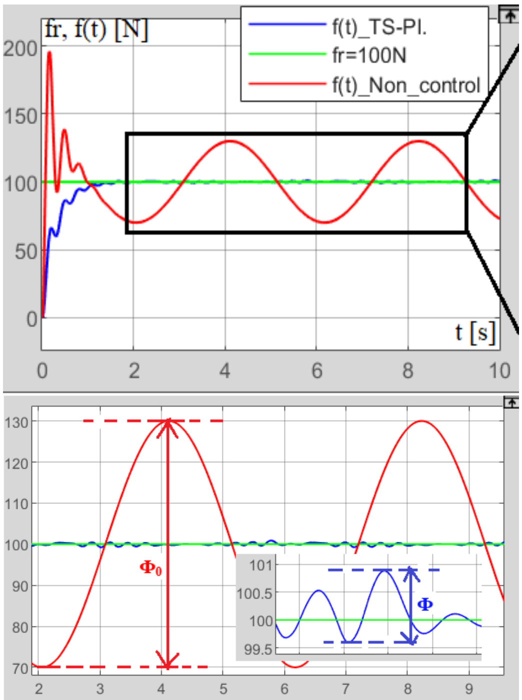

Fig. 9. The contact force regulation performance for the T-S fuzzy algorithm.

By comparing with the best MZL algorithm in [12], where VSE=83.59%, it can be found that the contact force regulation performance of the robust PI algorithm is the lowest one, and the contact force regulation performance of the modified T-S fuzzy algorithm is the best one. It should be noted that the time to obtain the steady state is the same, about 1.7s for all three control algorithms. The vertical position of the pantograph head $x_h(t)$ and uplift force $u(t)$ are illustrated in Figures 10-11.

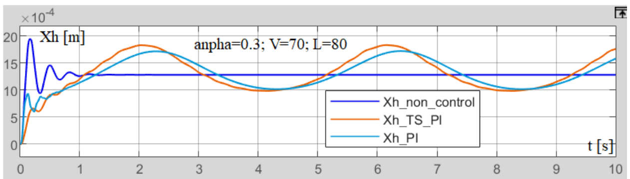

Fig. 10. Vertical position of the pantograph head $x_h(t)$.

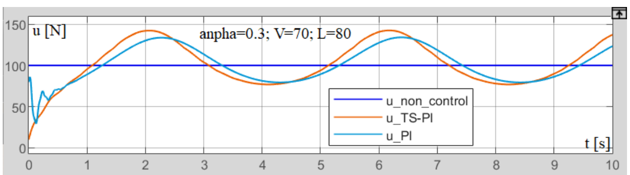

Fig. 11. Uplift force $u(t)$.

It can be seen that the T-S fuzzy algorithm uses a little larger uplift force than the robust PI algorithm. Some simulations were carried out to test the robustness of the proposed control algorithms. The cases in Figures 12-16 are first considered for the variations of the speed of train *V*, and the length in a span *L*.

(a)

(b)

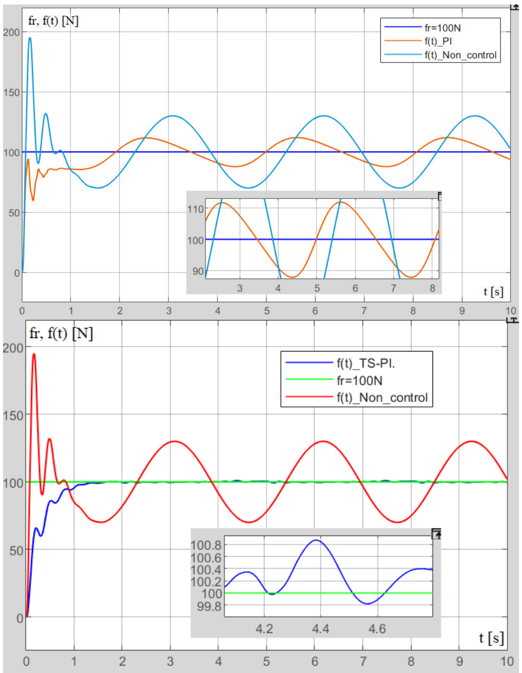

Fig. 12. Contact force relation performance for *V*=70, *L*=60: (a) Robust PI controller, (b) modified T-S fuzzy controller.

(a)

(b)

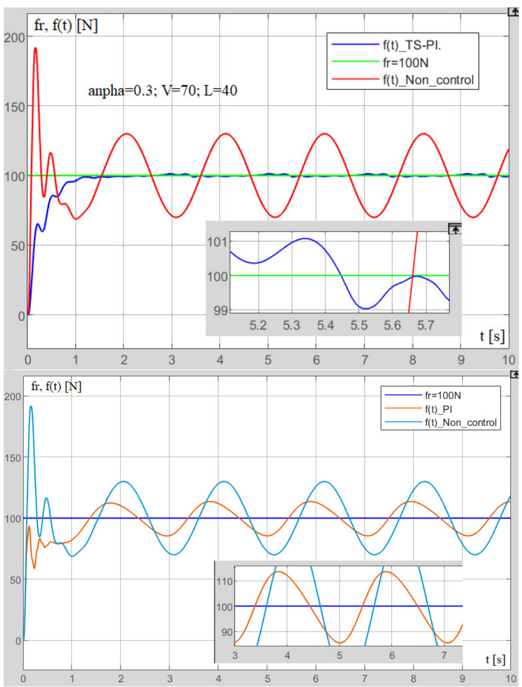

Fig. 13. Contact force regulation performance for *V*=70, *L*=40: (a) Robust PI controller, (b) modified T-S fuzzy controller.

(a)

(b)

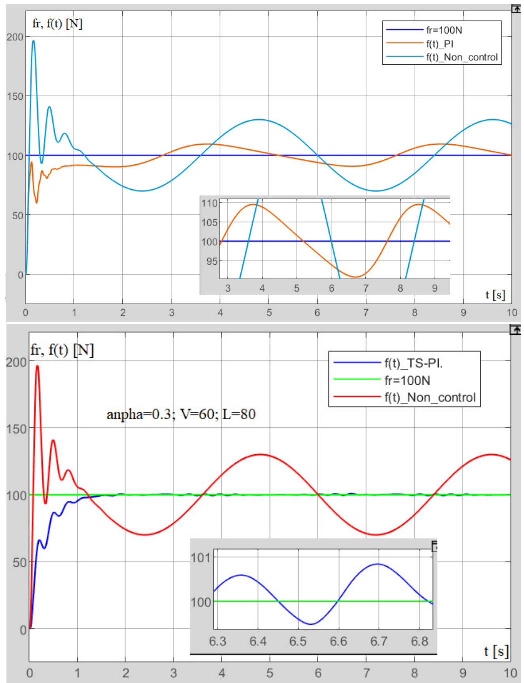

Fig. 14. Contact force relation performance for *V*=60, *L*=80: (a) Robust PI controller, (b) modified T-S fuzzy controller.

(a)

(b)

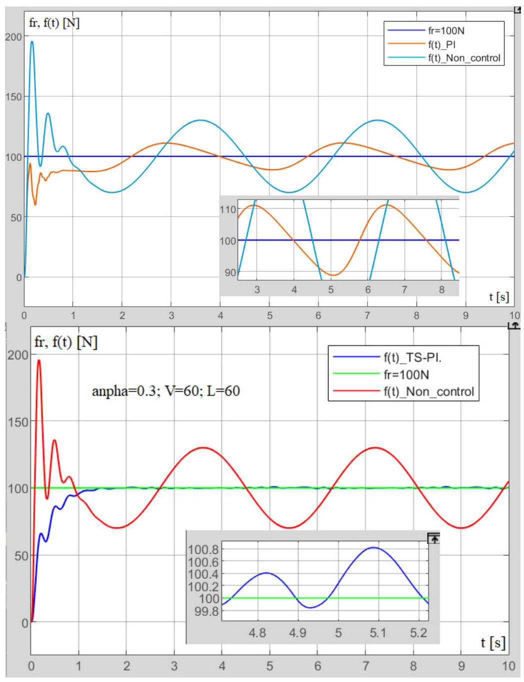

Fig. 15. Contact force regulation performance for *V*=60, *L*=60: (a) Robust PI controller, (b) modified T-S fuzzy controller.

The obtained results are given in Table I. They show that when the speed *V* and the length *L* vary, the vibration suppression efficiency for the modified T-S fuzzy controller is very high and stable. The reason is that although these parameters can vary, the boundary of $k \in [k_{min}, k_{\max}]$ is not changed.

(a)

(b)

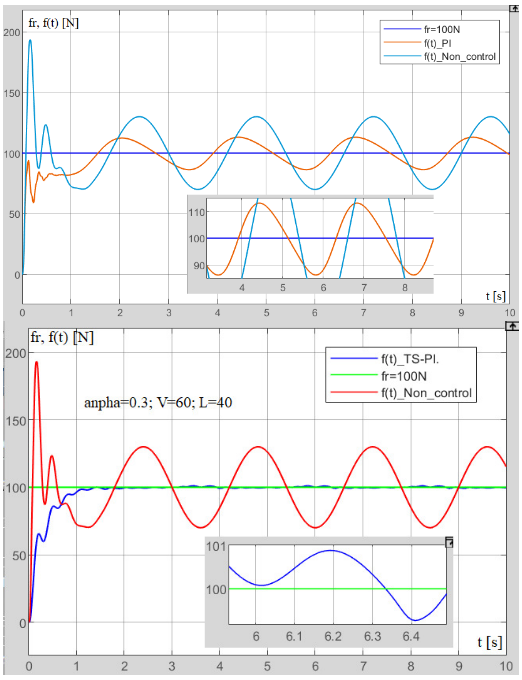

Fig. 16. Contact force regulation performance for *V*=60, *L*=40: (a) Robust PI controller, (b) modified T-S fuzzy controller.

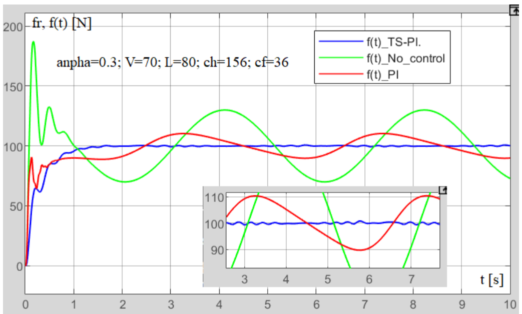

Fig. 17. Simulated parameters of $V=70$, $L=80$, $c_h+20\%$, $c_f+20\%$.

The performance of vibration suppression and contact force regulation, the stiffness of the viscous damping of the pan-head suspension c_h, and the frame suspension c_f were transformed by 80% to 120% of their nominal values given in the above simulation. The results are given in Figures 17-20.

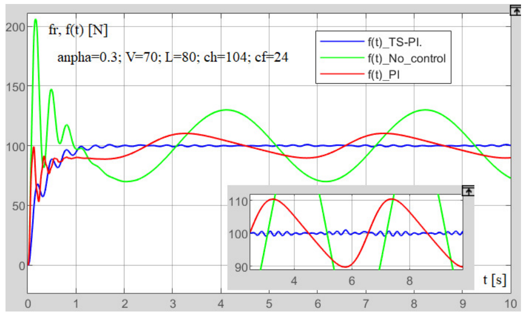

Fig. 18. Simulated parameters of $V=70$, $L=80$, $c_h+20\%$, $c_f+20\%$.

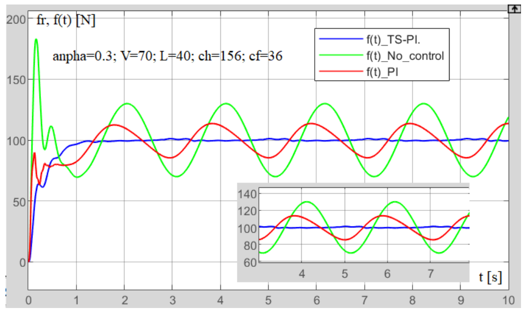

Fig. 19. Simulated parameters of $V=70$, $L=40$, $c_h+20\%$, $c_f+20\%$.

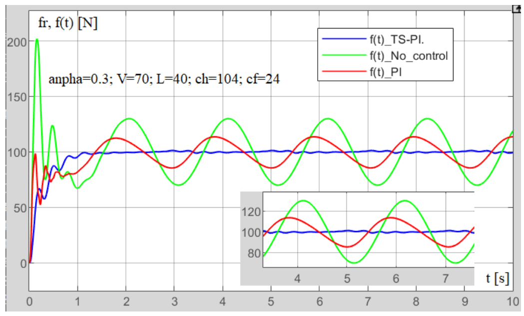

Fig. 20. Simulated parameters of $V=70$, $L=40$, $c_h-20\%$, $c_f-20\%$.

TABLE I. COMPARATIVE RESULTS OF THE VIBRATION SUPPRESSION EFFICIENCY FOR *a*=0.3

Time varying stiffness	***a***	0.3					
	V	60			70		
	L	40	60	80	40	60	80
PI	VSE (%)	55.39	63.01	68.80	53.16	59.80	65.66
MZL	VSE (%)	78.93	82.31	84.85	75.95	81.22	83.59
TS-PI	VSE (%)	97.35	98.36	97.74	96.58	98.25	97.68

TABLE II. TEST OF PERFORMANCE ROBUSTNESS

Item			**VSE (*a* = 0.3, *V* = 70, *L* = 80)**	**VSE (*a* = 0.3, *V* = 70, *L* = 40)**
Viscous damping coefficient c_h, c_f	**TS-PI**	+20%	98.0967%	96.8567%
		-20%	97.5241%	96.2175%
	PI	+20%	65.6442%	53.0810%
		-20%	65.6805%	53.2043%

VI. CONCLUSION

In this paper, a new robust intelligent control scheme has been successfully presented to suppress the vibration between the pantograph and the catenary by regulating the contact force to a reference value, hence, achieving a stable current collection. The proposed control method has some advantages. The T-S fuzzy model [15] used in this paper has some differences in comparison with the traditional T-S fuzzy model: differential equations are applied instead of the state model, and the consequents of the control rule have two parts, the numerator and the denominator of the control signal. This allows the description of the closed-loop T-S fuzzy control system as a polytope of linear systems so that the system stability analysis can be done, which is the main difficulty in many intelligent control methods, including fuzzy control.

Furthermore, the simple PID controllers are combined with fuzzy logic rules using the PDC design concept. The comparative simulation results have shown that the vibration of the contact force resulting from the time-varying stiffness of the catenary can be effectively suppressed. In particular, the proposed modified T-S fuzzy control algorithm is more efficient than the new intelligent control algorithm represented in [12] and the simple PI structure algorithm. Moreover, once the system stability is guaranteed, the proposed fuzzy controller is robust against possible changes in many system parameters: operational speed of train V, the length in a span L, and the stiffness of the viscous damping.

ACKNOWLEDGMENT

This research is supported by the University of Transport and Communications, Hanoi, Vietnam.

REFERENCES

[1] T. X. Wu and M. J. Brennan, "Active vibration control of a railway pantograph," *Proceedings of the Institution of Mechanical Engineers, Part F: Journal of Rail and Rapid Transit*, vol. 211, no. 2, pp. 117–130, Mar. 1997, https://doi.org/10.1243/0954409971530969.

[2] W. Shudong, G. Jingbo, and G. Guosheng, "Research of the active control for high-speed train pantograph," in *2008 IEEE Conference on Cybernetics and Intelligent Systems*, Chengdu, China, Sep. 2008, pp. 749–753, https://doi.org/10.1109/ICCIS.2008.4670754.

[3] H. Wei, C. D. Xu, and K. W. E. Cheng, "A short review on pantograph-catenary arcing issue in high-speed railway systems," in *The 11th IET International Conference on Advances in Power System Control, Operation and Management (APSCOM 2018)*, Hong Kong, China, Aug. 2018, pp. 1–4, https://doi.org/10.1049/cp.2018.1808.

[4] M. Simarro, S. Postigo, M. Prado-Novoa, A. Pérez-Blanca, and J. J. Castillo, "Analysis of contact forces between the pantograph and the overhead conductor rail using a validated finite element model," *Engineering Structures*, vol. 225, Dec. 2020, Art. no. 111265, https://doi.org/10.1016/j.engstruct.2020.111265.

[5] J. Baillieul and T. Samad, Eds., "Proportional-Integral-Derivative Control," in *Encyclopedia of Systems and Control*, London, UK: Springer, 2015, pp. 1103–1103, https://doi.org/10.1007/978-1-4471-5058-9_100019.

[6] P. Mahajan, R. Garg, V. Gupta, and P. Kumar, "Design of controller for pantograph-catenary system using reduced order model," in *2014 6th IEEE Power India International Conference (PIICON)*, Delhi, India, Sep. 2014, https://doi.org/10.1109/POWERI.2014.7117725.

[7] Z. Xiaodong and F. Yu, "Active self-adaptive control of high-speed train pantograph," in *2011 IEEE Power Engineering and Automation Conference*, Wuhan, China, Sep. 2011, vol. 3, pp. 152–156, https://doi.org/10.1109/PEAM.2011.6135036.

[8] Z. Liu, Y. Liu, N. Zhou, D. Zou, and H. Tu, "Backstepping Controller Design for Pantograph-Catenary System," *IOP Conference Series: Materials Science and Engineering*, vol. 428, no. 1, Jun. 2018, Art. no. 012045, https://doi.org/10.1088/1757-899X/428/1/012045.

[9] A. Ioan Chiriac, S. Constantin Olteanu, and D. Popescu, "Model Predictive Control Approach for a Pantograph-Catenary System (PAC) Described by a Transfer Function Model," in *2020 24th International Conference on System Theory, Control and Computing (ICSTCC)*, Sinaia, Romania, Jul. 2020, pp. 733–738, https://doi.org/10.1109/ICSTCC50638.2020.9259700.

[10] N. Mokrani and A. Rachid, "A robust control of contact force of pantograph-catenary for the high-speed train," in *2013 European Control Conference (ECC)*, Zurich, Switzerland, Jul. 2013, pp. 4568–4573, https://doi.org/10.23919/ECC.2013.6669668.

[11] Y. J. Huang and T. C. Kuo, "Discrete pantograph position control for the high speed transportation systems," in *IEEE International Conference on Networking, Sensing and Control, 2004*, Taipei, Taiwan, Mar. 2004, vol. 2, pp. 932-936 Vol.2, https://doi.org/10.1109/ICNSC.2004.1297072.

[12] T.-C. Lin, C.-W. Sun, Y.-C. Lin, and M. M. Zirkohi, "Intelligent Contact Force Regulation of Pantograph–Catenary Based on Novel Type-Reduction Technology," *Electronics*, vol. 11, no. 1, Jan. 2022, Art. no. 132, https://doi.org/10.3390/electronics11010132.

[13] M. Moradi Zirkohi and T.-C. Lin, "An efficient non-iterative method for computing the centroid of an interval type-2 fuzzy set," *Journal of Intelligent & Fuzzy Systems*, vol. 41, no. 2, pp. 2879–2889, Jan. 2021, https://doi.org/10.3233/JIFS-202913.

[14] N. Zerroug, K. Behih, Z. Bouchama, and K. Zehar, "Robust Adaptive Fuzzy Control of Nonlinear Systems," *Engineering, Technology & Applied Science Research*, vol. 12, no. 2, pp. 8328–8334, Apr. 2022, https://doi.org/10.48084/etasr.4781.

[15] L. H. Lan, P. Van Lam, and N. Van Hai, "An Approach to the Analysis and Design of Fuzzy Control System," in *2020 3rd International Conference on Robotics, Control and Automation Engineering (RCAE)*, Chongqing, China, Aug. 2020, pp. 36–40, https://doi.org/10.1109/RCAE51546.2020.9294179.

[16] C. Hwang, L. Hwang, and J. Hwang, "Robust D-partition," *Journal of the Chinese Institute of Engineers*, vol. 33, no. 6, pp. 811–821, Sep. 2010, https://doi.org/10.1080/02533839.2010.9671671.

[17] I. H. Hamad, A. Chouchaine, and H. Bouzaouache, "A Takagi-Sugeno Fuzzy Model for Greenhouse Climate," *Engineering, Technology & Applied Science Research*, vol. 11, no. 4, pp. 7424–7429, Aug. 2021, https://doi.org/10.48084/etasr.4291.

[18] T. Takagi and M. Sugeno, "Fuzzy identification of systems and its applications to modeling and control," *IEEE Transactions on Systems, Man, and Cybernetics*, vol. SMC-15, no. 1, pp. 116–132, Jan. 1985, https://doi.org/10.1109/TSMC.1985.6313399.

[19] H. O. Wang, K. Tanaka, and M. F. Griffin, "An approach to fuzzy control of nonlinear systems: stability and design issues," *IEEE Transactions on Fuzzy Systems*, vol. 4, no. 1, pp. 14–23, Oct. 1996, https://doi.org/10.1109/91.481841.

[20] L. K. Wong, F. H. F. Leung, and P. K. S. Tam, "Design of fuzzy logic controllers for Takagi–Sugeno fuzzy model based system with guaranteed performance," *International Journal of Approximate Reasoning*, vol. 30, no. 1, pp. 41–55, May 2002, https://doi.org/10.1016/S0888-613X(02)00062-2.

[21] M. Fu and B. R. Barmish, "Polytopes of Polynomials with Zeros in a Prescribed Region," in *1988 American Control Conference*, Atlanta, GA, USA, Jun. 1988, pp. 2461–2464, https://doi.org/10.23919/ACC.1988.4790138.